

Research Article

Primary Infection of BALB/c Mice with a Dengue Virus Type 4 Strain Leads to Kidney Injury

Arthur da Costa Rasinhas<sup>1,2</sup>, Fernanda Cunha Jácome<sup>1,2</sup>, Gabriela Cardoso Caldas<sup>1,3</sup>, Ana Luisa Teixeira de Almeida<sup>1</sup>, Daniel Dias Coutinho de Souza<sup>1</sup>, João Paulo Rodrigues dos Santos<sup>3</sup>, Helver Gonçalves Dias<sup>2</sup>, Eduarda Lima Araujo<sup>1</sup>, Ronaldo Mohana-Borges<sup>4</sup>, Ortrud Monika Barth<sup>1</sup>, Flavia Barreto dos Santos<sup>2</sup>, Debora Ferreira Barreto-Vieira<sup>1</sup>

<sup>1</sup>Laboratory of Viral Morphology and Morphogenesis, Oswaldo Cruz Institute, Fiocruz, Rio de Janeiro, RJ, Brazil; <sup>2</sup>Laboratory of Viral Immunology, Oswaldo Cruz Institute, Fiocruz, Rio de Janeiro, RJ, Brazil; <sup>3</sup>Laboratory of Pathology, Oswaldo Cruz Institute, Fiocruz, Rio de Janeiro, RJ, Brazil; <sup>4</sup>Laboratory of Biotechnology and Structural Bioengineering, Biophysics Institute Carlos Chagas Filho, Rio de Janeiro Federal University, Rio de Janeiro, RJ, Brazil.

Corresponding-author: rasinhas@protonmail.com

<https://orcid.org/0000-0002-6012-318X>

Received 06 November 2022

Accepted 07 March 2023

**Abstract:** Dengue is a disease caused by dengue virus (DENV-1 through -4), and is responsible for over 300 million cases worldwide. Among the four serotypes, DENV-4 remains the least studied, with limited data on the histopathology of the disease. Acute kidney injury is a potential complication of dengue generally associated with severe dengue infection. This reinforces the need for a better understanding of the consequences of dengue infection in renal tissue. Recently, the BALB/c mouse strain has gained ground as a competent model for experimental dengue infection. In this study,

BALB/c mice were infected through the intravenous route with a DENV-4 strain, isolated from a human patient. The kidneys of the mice were procured and subject to histopathological and ultrastructural analysis. The presence of the viral antigen was confirmed through immunohistochemistry. Analysis of tissue sections revealed the presence of inflammatory cell infiltrate throughout the parenchyma. Glomerular enlargement was a common find. Necrosis of tubular cells and hemorrhage were also observed. Analysis of the kidney on a transmission electron microscope allowed a closer look into the necrotic tubular cells, which presented nuclei with condensed chromatin, and loss of cytoplasm. Even though the kidney is probably not a primary target of dengue infection in mice, the inoculation of the virus in the blood appears to damage the renal tissue through local inflammation.

**Keywords:** DENV-4; BALB/c mice; Kidney; Histopathology; Ultrastructure

**Sponsorships:** This study was supported by Laboratory of Viral Morphology and Morphogenesis, IOC, Fiocruz, FIOTEC to Debora Ferreira Barreto Vieira [grant number IOC-023-FIO-18-2-58], Fundação de Amparo à Pesquisa do Estado do Rio de Janeiro [FAPERJ] to Flavia Barreto dos Santos [grant number E-26/202.003/2016], Conselho Nacional de Desenvolvimento Científico e Tecnológico (CNPq) to Flavia Barreto dos Santos [grant number 302462/2018-0] and Coordenação de Aperfeiçoamento de Pessoal de Nível Superior (CAPES) and CNPq for the student fellowships.

## **Introduction**

Dengue is a tropical febrile disease transmitted by mosquitoes of the *Aedes* genus and caused by each of the four serotypes of the dengue virus (DENV-1,-2,-3 and-4).<sup>(1)</sup> According to the World Health Organization, over 390 million infections occur every year, with 3.9 billion people living in areas with risk of transmission. The four serotypes circulate simultaneously in many countries, and, as of 2010, Brazil is listed among these countries, due to the reintroduction of DENV-4.<sup>(2,3)</sup> While

most cases of dengue remain mild or asymptomatic, one in twenty cases evolve to what is called severe dengue (SD), a condition closely associated with intense hemorrhage, plasma leakage and multiple organ impairment.<sup>(4,5)</sup> Even though the liver is the most commonly affected organ<sup>(6,7)</sup>, DENV has been shown to infect a wide range of biological tissues, such as the lungs<sup>(8)</sup>, the heart<sup>(9)</sup>, the brain<sup>(10)</sup> and even the kidneys<sup>(11)</sup>, among others.

Thus far, the alterations caused by DENV infection in the kidney remain largely unexplored, despite reports of signs and symptoms such as proteinuria, hematuria, glomerulonephritis, nephrotic syndrome and elevation of serum creatinine levels.<sup>(12-14)</sup> More severe manifestations, such as acute kidney injury (AKI), rhabdomyolysis, glomerulonephritis, hemolytic uremic syndrome, and acute renal failure, are often associated to lethal cases of SD.<sup>(11,15,16)</sup> Histopathological alterations described in renal tissue include congestion of the glomerular capillary, focal hemorrhage, edema, inflammatory cell infiltration, hydropic degeneration, formation of micro abscesses, thrombus formation in the glomeruli, glomerular congestion and acute necrosis of proximal and distal tubules.<sup>(6,17-22)</sup> On an ultrastructural level, these necrotic tubular cells were shown to be undergoing pyknosis, with dilated endoplasmic reticulum.<sup>(6)</sup> DENV like particles have already been directly observed in the kidney through transmission electron microscopy, suggesting viral infection.<sup>(17)</sup> Viral antigens have also been previously detected in the kidney, in tubular cells<sup>(23)</sup>, in inflammatory cells<sup>(24)</sup>, in glomerular endothelial cells, in mesangial cells<sup>(21,22)</sup>, in hematopoietic cells<sup>(25)</sup> and in circulating macrophages and monocytes.<sup>(6)</sup> Additionally, the detection of DENV RNA through molecular technique has been reported in kidney.<sup>(8)</sup>

AKI is a renal manifestation of dengue that is often reported in the literature. This condition is characterized by a sudden decrease of kidney function, which can culminate in death.<sup>(12)</sup> The severity of dengue increases the risk of AKI, with it being reported in 11.8% of patients with dengue with warning signs and in 28.6% of patients with SD.<sup>(26)</sup> Around 10 to 20% of patients presenting

dengue-induced AKI may require dialysis following the resolution of the disease.<sup>(27)</sup> Despite this, dengue-induced AKI remains a poorly explored manifestation.<sup>(28-30)</sup> The histopathology of AKI is characterized by proximal and distal tubule necrosis, with lumen dilation, loss of the brush border, simplification of the tubular lining epithelium, and loss of nuclei.<sup>(31)</sup> Although the mechanisms that lead to AKI are not yet fully understood, its appearance is hypothesized to be due to a series of factors, such as the direct cytopathic viral action, cytokine induced hemodynamical alterations, deposition of antigen-antibody immune complexes, rhabdomyolysis, hemolysis and acute glomerular injury.<sup>(13,16,27,32)</sup>

Over the years, the BALB/c mouse has proven itself to be a useful animal model for dengue infection studies, replicating many aspects of the disease as it manifests in human cases. These animals not only present immune response against DENV, but also manifest histopathological alterations in liver, lung, heart, kidney, brain, spleen and skeletal muscle.<sup>(33-43)</sup> Furthermore, currently, DENV-4 remains the least studied serotype of DENV, with most studies focusing on serotype 2.<sup>(40)</sup> Since DENV-4 is known to cause milder cases of dengue<sup>(44)</sup>, it is unclear whether the kidney is a target organ for infection. While few studies focus on the renal manifestations caused by dengue in BALB/c mice, alterations such as an increase in glomerular volume and in mesangial cellularity, inflammatory cell infiltration, peritubular congestion, tubular necrosis, loss of brush border microvilli, cytoplasmic loss, glomerular atrophy and focal hemorrhage have been previously reported.<sup>(45,46)</sup> The viral antigen has also been successfully detected in DENV-infected mouse kidney, in tubular epithelial cells and in endothelial cells.<sup>(46)</sup>

Given the scarcity of data on AKI in humans and the lack of histopathological studies on kidney, this study aims to investigate the renal manifestations of dengue in BALB/c mice infected with DENV-4.

## Materials and Methods

**Ethics statement.** All the procedures performed during the course of this study were in compliance with the principles and regulations established by the Brazilian College of Animal Experimentation and previously approved by the Animal Ethics Committee of Oswaldo Cruz Institute (IOC), Oswaldo Cruz Foundation (Fiocruz), under protocol number L-023/2018.

**Viral strain.** The DENV-4 strain BR2972/2013, isolated from a patient's serum, was used in this study. Serotype was identified by Real Time Quantitative RT-PCR<sup>(47)</sup> and by isolation into *Aedes albopictus* cell line (C6/36 cells; accession number: CRL-1660)<sup>(48)</sup>, performed by the Flavivirus Laboratory, Fiocruz. A sample was kindly provided for use in this study.

**Viral stock production.** The viral stock was prepared by inoculating the DENV-4 strain BR2972/2013 into 175 cm<sup>2</sup> culture cell flasks containing *Aedes albopictus* C6/36 cells<sup>(48)</sup> at a concentration of  $5 \times 10^5$  cells/mL. Briefly, for virus propagation, *Aedes albopictus* C6/36 cells were grown in Leibovitz medium (L-15, Sigma-Aldrich Corporation, USA) with 10% fetal bovine serum (Gibco, Thermo Fisher Scientific Inc., USA) in an incubator at 28°C. Prior to virus inoculation, L-15 medium was replaced, 2% fetal bovine serum was added and 100 µL of the DENV-4 strain was inoculated and incubated at 28°C for 5 days. The virus was harvested by transferring all the flask supernatant to a 15 mL centrifuge tube, centrifuging for 10 min at 4000 x g at 4°C. Supernatant aliquots were stored at -70°C for titration. After three cell passages, the strain presented a viral titer of  $10^9$  TCID<sub>50</sub>/mL, and was used for experimental infection. The viral titer was calculated using the Reed Muench method.<sup>(49)</sup>

**Study design.** For this study, thirty mice were used. Fifteen kidney samples were subject to analysis through bright field microscopy, with ten mice being infected with DENV-4 and five mice uninfected, used as mock-infected control. Another fifteen were subject to transmission electron microscopy

analysis, following the same aforementioned criteria of ten infected and five uninfected, with one kidney destined to ultrastructural analysis, and the remaining kidney for qRT-PCR analysis.

**Experimental infection.** For experimental infection with DENV-4, two months-old male BALB/c mice, provided by the Institute of Science and Technology in Biomodels, at Fiocruz, Rio de Janeiro, Brazil, were used. During the experimentation period, the mice were housed in the vivarium of Hélio and Peggy Pereira Pavilion, IOC, Fiocruz (biosafety level 2), and separated in groups of five per cage. Mice were inoculated through the caudal vein with 100  $\mu$ L of the DENV-4 strain diluted in L-15 medium, which presented a viral titer of 10000 TCID<sub>50</sub>/0.1 mL. For the negative control, mice were inoculated with 100  $\mu$ L of centrifuged C6/36 cell culture supernatant in L-15 culture medium (Sigma-Aldrich Corporation, USA). All the mice were euthanized 72 hours post infection. Euthanasia was performed using a lethal dose of ketamine (150 mg/kg), xylazine (10 mg/kg) and tramadol (10 mg/kg), administered through the intraperitoneal route. Once the anesthetic effect set in, the mice were subject to cervical dislocation and the organs were harvested.

**Bright field microscopy.** Following the organ harvest, the collected kidneys were placed on a glass plate, and sectioned along the sagittal plane, in two equal halves. Afterwards, the samples were and stored in a histological cassette, and placed in a container containing Millonig's buffered formalin. Subsequently, the tissue was dehydrated in baths of increasing concentrations of ethanol, clarified in xylene and embedded in paraffin. Tissue sections 5 $\mu$ m thick were obtained using a Leica 2025 microtome (Leica, Germany) and stained with hematoxylin and eosin. Finally, the stained glass slides were analysed on a bright field microscope (AxioHome, Zeiss, Germany).

**Histomorphometry.** Glomeruli count and glomerular area were measured on kidney samples of BALB/c mice. Ten glass slides containing kidney histological sections stained with H&E (Five from mice infected with DENV-4 and five from uninfected mice, of the mock-infected control group) were

analysed on a bright field microscope (AxioHome, Zeiss, Germany). For each glass slide, 20 images of random areas were captured at 200 magnification using a coupled camera. For each image, all glomeruli were counted and had their area quantified using the open-source image analysis software ImageJ.

**Statistical analysis.** A database on the glomeruli count and glomerular area of infected and uninfected mice was created in Microsoft Excel and the mean of the values was calculated. The resulting data was analysed using the GraphPad Prism software version 8.0.1 and the SPSS Statistics software version 25. The Shapiro-Wilk test ( $p > 0.05$ ) was used to assess the normality of data. The Student's t-test was performed since the data followed a normal distribution and all results of  $p \leq 0.05$  were considered statistically significant.

**Immunohistochemistry.** Following deparaffinization and rehydration, the kidney samples underwent antigen retrieval, while submerged in EnVision Flex target retrieval solution, high pH (Dako, USA), inside a pressure cooker. Afterwards, a solution of hydrogen peroxidase in methanol was used, to block endogenous peroxidase. Samples were incubated with either anti-NS3 antibody produced in rabbit (1:200), provided by the Laboratory of Biotechnology and Structural Bioengineering, of the Rio de Janeiro Federal University or anti-flavivirus envelope protein antibody produced in mouse (1:200), provided by the Flavivirus Laboratory, IOC, Fiocruz. Finally, samples were incubated with anti-rabbit antibody horseradish peroxidase conjugate (Advanced Biosystems, USA). Reaction was revealed with diaminobenzidine (Scytek, USA) as chromogen and sections were counterstained with Harris's hematoxylin (Dako, USA). A reaction control was performed using only the secondary horseradish peroxidase-conjugated antibody.

**Transmission electron microscopy.** Kidney samples were fixated in 3% glutaraldehyde in sodium cacodylate buffer 0.2 M, pH 7.2, stored at 4°C and processed as described by Barreto-Vieira.<sup>(50)</sup> The

resulting resin blocks were sliced in ultrathin sections 50-70 nm thick with a Reichert-Jung Ultracut E ultramicrotome (Leica, Germany) and placed on copper grids. These sections were then analysed on a Hitachi HT 7800 transmission electron microscope (Hitachi, Japan).

**Real Time Quantitative RT-PCR.** For molecular analysis, kidneys were washed with phosphate buffered saline and store at -80°C. The samples were macerated in L-15 culture medium (Invitrogen, USA) and centrifuged for fifteen minutes at 10000 rpm at 4°C. Extraction was performed with 140 µL of kidney macerate supernatant, with the QIAmp Viral RNA mini kit (Qiagen, Germany), following the protocol described by the manufacturer. Amplification was performed using the SuperScript III Platinum One-Step Quantitative RT-PCR kit (Invitrogen Corporation, USA) according to the kit's instructions, using the primers DENJ-4R (5'TCCACCTGAGACTCCTTCCA3') and DENJ-4F (5'TTGTCCTAATGATGCTGGTCG3'), and probe DENJ-4P (6-FAM 5'TTCCTACTCCTACGCATCGATTCCG3' BHQ-1).<sup>(47)</sup> Reaction was performed in a 7500 Real-Time PCR System (Applied Biosystems, USA).

## Results

**Histopathological, histomorphometrical and ultrastructural alterations.** Mice of the mock-infected control group showed no signs of kidney injury. The glomeruli presented a regular aspect, with normal sized cells and well-defined parietal and visceral layers. Tubular cells also presented no histopathological alterations. Renal tubules had a healthy appearance, with well-preserved lumen and brush border (Figure 1A, B). Mice infected with DENV-4, on the other hand, showed a noticeable decrease of the area of the Bowman's Space, due to an apparent increase in the glomerular cellularity (Figure 1C), oftentimes making it impossible to distinguish the visceral and parietal layers. In some kidney sections where the Bowman's space was preserved, erythrocytes were observed within, between the layers of the capsule (Figure 1D). Clear vacuoles were seen in the cytoplasm of tubular



cells, some causing the lateralization of the nucleus (Figure 1C). The presence of inflammatory infiltrate was discrete, but ubiquitous, represented by small but noticeable clusters of inflammatory cells in the tubular interstice (Figure 1C, D). Capillary edema was also observed, although not a common find (Figure 1D). Distal and proximal convoluted tubules going through different stages of necrosis were present in the tissue (Figure 1E). Small hemorrhagic foci were present throughout the kidney, both in the medullar and cortical regions (Figure 1E, F). Larger hemorrhagic areas were present only in the kidney of a mouse that tested positive for DENV-4 envelope protein (Figure 2A). Blood was present not only in the tubular interstice (Figure 2B), but also in the lumen of the thin part of the loop of Henle (Figure 2C, D). The frequency of each histopathological finding is depicted in table I.

A statistically significant ( $p = 0.0451$ ) decrease in the glomerular count per analyzed kidney was observed in DENV-4 infected mice (Figure 3A). Glomerular area was also smaller in DENV-4 infected mice, although this alteration was not statistically significant (Figure 3B).

Upon ultrastructural inspection, uninfected kidneys showed no morphological alterations, both in the tubular and in the glomerular structure. Glomerular integrity was well preserved, with a clear distinction of the Bowman's space and its layers. (Figure 4A, B). Analysis of the kidneys of mice infected with DENV-4 offered a closer look into the necrotic process of the tubular cells, which presented intense loss of cytoplasm and condensation of the chromatin within the nucleus, characteristic of pyknosis (4C, E). Loss of the microvilli that forms the brush border of the proximal convoluted tubule was also observed (Figure 4C). Vacuoles of unknown origin, smaller than the other described during bright field microscopy analysis, and filled with a substance unlike water or lipids, were observed inside cells of the distal convoluted tubule, more commonly present in the apical region of necrotic cells (Figure 4D). In the glomeruli, Bowman's space was reduced, seemingly due to an expansion of the mesangial matrix of mesangial cells. Capillary lumen was also noticeably reduced

(Figure 4F). Inflammatory cells were identified circulating in renal the capillaries and in the tubular interstice, and consisted mostly of lymphocytes (Figure 5A) and neutrophils (Figure 5B).

**Antigen and viral genome detection.** No immunostaining was observed in mice of the control group (Figure 6A, B). Reaction control also did not show any immunostaining. While the NS3 antigen was not detected in any of the tested kidneys, the envelope protein was detected in the cortical region, in cells of the proximal convoluted tubule (Figure 6C), in its lumen (Figure 6E) and in the endothelium of capillaries (Figure 6D). In the medullar region, immunostaining was observed in cells of the loop of Henle (Figure 6F). The envelope protein was detected in 4 out of 8 (50%) tested kidney samples. DENV-4 viral RNA was not detected in any of the mice kidneys tested through qRT-PCR.

## Discussion

Overall, the results described in this study are in line with what is seen in human cases of dengue presenting renal manifestations. Histopathological alterations observed fit the descriptions of dengue-induced AKI published in the related literature<sup>(13,16)</sup>, albeit milder, and non-lethal.

Vascular alterations induced by DENV seem to be the main cause for acute tubular necrosis, due to a decrease in renal perfusion, which in turn leads to ischemia.<sup>(51)</sup> Rhabdomyolysis, a muscular manifestation of DENV infection, while seemingly unrelated to kidney injury, also plays a large role in the development of acute tubular necrosis during dengue. This condition is characterized by the necrosis of skeletal muscle cells, resulting in the release of proteins in the circulation. One of these proteins, myoglobin, is known to deposit in the renal tubules, causing tubular injury and tubular obstruction.<sup>(11,28)</sup> The loss of microvilli described here could represent the initial stages of proximal convoluted tubule necrosis, characterized by loss of the brush border.<sup>(31)</sup> Even though some tubular cells appeared to be undergoing necrosis, the process did not seem widespread, and could perhaps be self-limited, reversible even, following the resolution of the disease. The vacuoles observed in tubular

cells of the cortical region through bright field microscopy, though remarkable, are not completely unusual, at least in male mice. Even if these vacuoles were not perceived in mice of the control group, their appearance is said to be benign, and not a major histopathological find.<sup>(52)</sup> The smaller unidentified vacuoles, however, were only observed through transmission electron microscopy, and could be a direct result of the necrosis of the cells, since they were only seen in necrotic cells, in cellular regions suffering from loss of cytoplasm.

While Póvoa et al.<sup>(6)</sup> did not detect the viral NS3 antigen in the kidney of human fatal cases of dengue, nor the presence of viral RNA, they did observe antigens hypothesized to be either the envelope or the membrane proteins in monocytes and macrophages. Jessie et al.<sup>(23)</sup> have also detected DENV antigens in tubular cell epithelium, with the absence of viral RNA in the renal tissue. Both authors suggest that this could be due to these different cell types reabsorbing the circulating immune complexes, with the same happening during yellow fever infection.<sup>(23)</sup> The deposition of immune complexes has been described in the glomeruli of BALB/c mice<sup>(53)</sup> and the presence of glomerular immune complex deposits has been associated to mesangial cell hypertrophy, observed through transmission electron microscopy.<sup>(54)</sup> Wiwanitkit<sup>(55)</sup> has suggested that, due to the size difference between the dengue virus-immunoglobulin immune complex and the glomerular capillary – the latter being much larger than the former – entrapment of the immune complex in the glomerulus should not easily happen, unless there is a significant narrowing of the glomerular diameter, due to lesion or infection.

In this study, although DENV RNA was not detected in kidney, the envelope protein was present in tubular cells and tubular lumen, cells of the loop of Henle and endothelium wall, suggesting that viral antigen reabsorption is likely to happen in the tubular pathway, should immune complexes end up being filtered by the glomerulus. Endothelial cells, on the other hand, are known to play a major role in the pathogenesis of dengue.<sup>(56)</sup> Some authors have previously suggested that the

envelope protein is capable of modifying the vascular permeability of the endothelium, either directly, altering the morphology of endothelial cells<sup>(57)</sup>, or through the infection of monocytes, which, in turn, contribute to viral replication and production of nitric oxide and cytokines, and, consequently, to an increase in endothelial permeability.<sup>(58)</sup> Cytokines and chemokines are also known to damage the tissue, being secreted by macrophages and T lymphocytes during the attempt to contain the viral infection.<sup>(59, 60)</sup> The cytokines IL-17 and IL-18, in particular, seem to be widely expressed in the kidney during severe cases of dengue.<sup>(19)</sup> In a recent study, Oliveira *et al.*, (2022) successfully detected the NS3 antigen in the kidney of fatal dengue cases in children. The presence of the viral antigen in mesangial and endothelial cells of the glomerulus, and in monocytes and macrophages, suggests that viral infection and replication can occur in the kidney in severe cases of dengue.<sup>(61)</sup>

Also described in this study was the increased size of the glomeruli, better observed through transmission electron microscopy. This alteration is the result of the expansion of the mesangial matrix of mesangial cells, leading not only to a decrease in the area of the Bowman's space, through where the glomerular filtrate flows, but also to the compression of the glomerular capillaries, possibly diminishing filtration rates, and facilitating the entrapment of immune complexes. Although the virus was not detected in kidney, the envelope protein was present. This could be a result of the circulation of the virus in the blood. Like Jácome *et al.*<sup>(46)</sup>, we also observed a decrease in glomeruli count in each analyzed kidney, suggesting the possibility of glomerular atrophy. Curiously, histomorphometrical data showed an actual decrease in glomerular area. While these results conflict with what was seen during histopathological and ultrastructural analysis, they were not statistically significant. Alterations in the kidney function are also linked to glomerular injury, and are often reported during dengue. These are associated to several biochemical imbalances, such as the increase of blood urea nitrogen and blood creatinine levels, both in BALB/c mice and in humans.<sup>(6, 27, 41, 62)</sup>

Hemorrhage and vascular leakage are hallmarks of dengue and SD, probably induced by cytokines. TNF $\alpha$ , IL6 and IL8 are known to alter the vascular permeability of capillaries, triggering cases of vascular leakage in dengue.<sup>(63)</sup> The reduced blood flow to the kidney likely leads to an ischemic process, and is the reason for the necrosis of tubular cells.<sup>(6)</sup> The presence of blood in later portions of the nephron suggests alterations in the kidney filtering capabilities. Furthermore, the increase of vascular permeability induced by DENV infection could also alter the filtration process, facilitating the passage of blood through the glomerular endothelium and onto the renal tubules. The areas of hemorrhage seen in the tubular interstice also indicate the occurrence of these hemodynamic alterations, reinforced by the presence of the viral antigen in the endothelial wall. Although blood was never directly observed in the urine of mice upon clinical inspection, the possibility of microscopic hematuria remains.<sup>(64)</sup> Larger hemorrhagic areas in kidneys positive for the envelope protein could indicate a correlation between the presence of the viral antigen and hemorrhage severity. An interesting perspective for a similar study would be the analysis of mice urine through urinalysis, to investigate the presence of proteinuria or hematuria.

The histopathological alterations observed in this study seemed much milder than those observed by Jácome et al..<sup>(46)</sup> This could be due to the simple fact that DENV-4 causes a less severe disease, when compared to other DENV serotypes.<sup>(44)</sup> Another possibility is that the kidney is not a primary target of dengue infection in mice, at least not under normal circumstances. This is not to say that infection of the kidney does not happen, just that it is less likely during a primary DENV infection. Nonetheless, the inoculation of the virus in the blood is enough to cause damage to the renal tissue, either through the action of cytokines, of circulating immune complexes and/or due to vascular permeability alterations. In the end, as is with all topics surrounding the pathogenesis of dengue, much is yet to be uncovered.

**Acknowledgments:** The authors would like to thank IOC for providing us with its technology and facilities during the course of the research, the Flavivirus Laboratory, IOC, Fiocruz, for providing the DENV-4 strain used in this study and the Laboratory of Pathology, IOC, Fiocruz for the support in sample processing and technical analysis.

## References

1. Martina BE, Koraka P, Osterhaus AD. Dengue virus pathogenesis: an integrated view. *Clin Microbiol Rev.* 2009 Oct;22(4):564-81. doi: 10.1128/CMR.00035-09. PMID: 19822889; PMCID: PMC2772360.
2. World Health Organization. Dengue and severe dengue [homepage on the Internet]. [updated 2022 January 10; cited 2022 August 7] Available from: <https://www.who.int/news-room/fact-sheets/detail/dengue-and-severe-dengue>.
3. Temporão JG, Penna GO, Carmo EH, Coelho GE, do Socorro Silva Azevedo R, Teixeira Nunes MR et al. Dengue virus serotype 4, Roraima State, Brazil. *Emerg Infect Dis.* 2011 May;17(5):938-40. doi: 10.3201/eid1705.101681. PMID: 21529421; PMCID: PMC3321786.
4. Guzman MG, Gubler DJ, Izquierdo A, Martinez E, Halstead SB. Dengue infection. *Nat Rev Dis Primers.* 2016 Aug 18;2:16055. doi: 10.1038/nrdp.2016.55. PMID: 27534439.
5. Centers for Disease Control and Prevention. Dengue: Symptoms and Treatment. [updated 2021 September 20; cited 2022 August 28] Available from: <https://www.cdc.gov/dengue/symptoms/index.html>.
6. Póvoa TF, Alves AM, Oliveira CA, Nuovo GJ, Chagas VL, Paes MV. The pathology of severe dengue in multiple organs of human fatal cases: histopathology, ultrastructure and virus replication.

PLoS One. 2014 Apr 15;9(4):e83386. doi: 10.1371/journal.pone.0083386. PMID: 24736395; PMCID: PMC3987999.

7. Fernando S, Wijewickrama A, Gomes L, Punchihewa CT, Madusanka SD, Dissanayake H et al. Patterns and causes of liver involvement in acute dengue infection. *BMC Infect Dis.* 2016 Jul 8;16:319. doi: 10.1186/s12879-016-1656-2. PMID: 27391896; PMCID: PMC4938910.

8. Cunha MDP, Duarte-Neto AN, Pour SZ, Hajjar LA, Frassetto FP, Dolhnikoff M et al. Systemic dengue infection associated with a new dengue virus type 2 introduction in Brazil - a case report. *BMC Infect Dis.* 2021 Apr 1;21(1):311. doi: 10.1186/s12879-021-05959-2. PMID: 33794785; PMCID: PMC8015031.

9. Mansanguan C, Hanboonkunupakarn B, Muangnoicharoen S, Huntrup A, Poolcharoen A, Mansanguan S et al. Cardiac evaluation in adults with dengue virus infection by serial echocardiography. *BMC Infect Dis.* 2021 Sep 10;21(1):940. doi: 10.1186/s12879-021-06639-x. PMID: 34507547; PMCID: PMC8431916.

10. Pandeya A, Upadhyay D, Oli B, Parajuli M, Silwal N, Shrestha A et al. Dengue encephalitis featuring "double-doughnut" sign - A case report. *Ann Med Surg (Lond).* 2022 Jun 5;78:103939. doi: 10.1016/j.amsu.2022.103939. PMID: 35734672; PMCID: PMC9207141.

11. Arif A, Abdul Razzaque MR, Kogut LM, Tebha SS, Shahid F, Essar MY. Expanded dengue syndrome presented with rhabdomyolysis, compartment syndrome, and acute kidney injury: A case report. *Medicine (Baltimore).* 2022 Feb 18;101(7):e28865. doi: 10.1097/MD.00000000000028865. PMID: 35363190; PMCID: PMC9281986.

12. Lombardi R, Yu L, Younes-Ibrahim M, Schor N, Burdmann EA. Epidemiology of acute kidney injury in Latin America. *Semin Nephrol.* 2008 Jul;28(4):320-329. doi: 10.1016/j.semnephrol.2008.04.001. PMID: 18620955.
13. Oliveira JF, Burdmann EA. Dengue-associated acute kidney injury. *Clin Kidney J.* 2015 Dec;8(6):681-5. doi: 10.1093/ckj/sfv106. Epub 2015 Oct 16. PMID: 26613023; PMCID: PMC4655808.
14. Begum F, Das S, Mukherjee D, Mal S, Ray U. Insight into the Tropism of Dengue Virus in Humans. *Viruses.* 2019 Dec 9;11(12):1136. doi: 10.3390/v11121136. PMID: 31835302; PMCID: PMC6950149.
15. Mehra N, Patel A, Abraham G, Reddy YN, Reddy YN. Acute kidney injury in dengue fever using Acute Kidney Injury Network criteria: incidence and risk factors. *Trop Doct.* 2012 Jul;42(3):160-2. doi: 10.1258/td.2012.120023. Epub 2012 Apr 3. PMID: 22472317.
16. Bignardi PR, Pinto GR, Boscaroli MLN, Lima RAA, Delfino VDA. Acute kidney injury associated with dengue virus infection: a review. *J Bras Nefrol.* 2022 Apr-Jun;44(2):232-237. doi: 10.1590/2175-8239-JBN-2021-0221. PMID: 35212704; PMCID: PMC9269180.
17. Limonta D, Falcón V, Torres G, Capó V, Menéndez I, Rosario D et al. Dengue virus identification by transmission electron microscopy and molecular methods in fatal dengue hemorrhagic fever. *Infection.* 2012 Dec;40(6):689-94. doi: 10.1007/s15010-012-0260-7. Epub 2012 Apr 20. PMID: 22527878.
18. Repizo LP, Malheiros DM, Yu L, Barros RT, Burdmann EA. Biopsy proven acute tubular necrosis due to rhabdomyolysis in a dengue fever patient: a case report and review of literature. *Rev Inst Med*



Trop Sao Paulo. 2014 Jan-Feb;56(1):85-8. doi: 10.1590/S0036-46652014000100014. PMID: 24553615; PMCID: PMC4085823.

19. Pagliari C, Simões Quaresma JÁ, Kanashiro-Galo L, de Carvalho LV, Vitoria WO, da Silva WL et al. Human kidney damage in fatal dengue hemorrhagic fever results of glomeruli injury mainly induced by IL17. J Clin Virol. 2016 Feb;75:16-20. doi: 10.1016/j.jcv.2015.12.005. Epub 2015 Dec 23. PMID: 26741825.

20. Ahsan J, Ahmad SQ, Rafi T. Postmortem Findings in Fatal Dengue Haemorrhagic Fever. J Coll Physicians Surg Pak. 2018 Jun;28(6):S137-S139. doi: 10.29271/jcpsp.2018.06.S137. PMID: 29866250.

21. Nunes PCG, Rioja LDS, Coelho JMCO, Salomão NG, Rabelo K, José CC et al. Renal Injury in DENV-4 Fatal Cases: Viremia, Immune Response and Cytokine Profile. Pathogens. 2019 Nov 7;8(4):223. doi: 10.3390/pathogens8040223. PMID: 31703246; PMCID: PMC6963280.

22. Cunha MS, de Moura Coletti T, Guerra JM, Ponce CC, Fernandes NCCA, Résio RA et al. A fatal case of dengue hemorrhagic fever associated with dengue virus 4 (DENV-4) in Brazil: genomic and histopathological findings. Braz J Microbiol. 2022 Jul 2. doi: 10.1007/s42770-022-00784-4. Epub ahead of print. PMID: 35779208.

23. Jessie K, Fong MY, Devi S, Lam SK, Wong KT. Localization of dengue virus in naturally infected human tissues, by immunohistochemistry and in situ hybridization. J Infect Dis. 2004 Apr 15;189(8):1411-8. doi: 10.1086/383043. Epub 2004 Apr 5. PMID: 15073678.

24. Basílio-de-Oliveira CA, Aguiar GR, Baldanza MS, Barth OM, Eyer-Silva WA, Paes MV. Pathologic study of a fatal case of dengue-3 virus infection in Rio de Janeiro, Brazil. Braz J Infect

Dis. 2005 Aug;9(4):341-7. doi: 10.1590/s1413-86702005000400012. Epub 2005 Nov 1. PMID: 16270128.

25. Bhoopat L, Bhamarapavati N, Attasiri C, Yoksarn S, Chaiwun B, Khunamornpong S et al. Immunohistochemical characterization of a new monoclonal antibody reactive with dengue virus-infected cells in frozen tissue using immunoperoxidase technique. *Asian Pac J Allergy Immunol.* 1996 Dec;14(2):107-13. PMID: 9177824.

26. Ismail J, Sankar J. Acute Kidney Injury in Dengue - Not Unprecedented. *Indian J Pediatr.* 2020 Dec;87(12):993-994. doi: 10.1007/s12098-020-03529-z. Epub 2020 Oct 16. PMID: 33063275.

27. Mallhi TH, Sarriff A, Adnan AS, Khan YH, Hamzah AA, Jummaat F et al. Dengue-induced Acute Kidney Injury (DAKI): A Neglected and Fatal Complication of Dengue Viral Infection - A Systematic Review. *J Coll Physicians Surg Pak.* 2015 Nov;25(11):828-34. PMID: 26577971.

28. Tansir G, Gupta C, Mehta S, Kumar P, Soneja M, Biswas A. Expanded dengue syndrome in secondary dengue infection: A case of biopsy proven rhabdomyolysis induced acute kidney injury with intracranial and intraorbital bleeds. *Intractable Rare Dis Res.* 2017 Nov;6(4):314-318. doi: 10.5582/irdr.2017.01071. PMID: 29259863; PMCID: PMC5735288.

29. Diptyanusa A, Phumratanapapin W. Predictors and Outcomes of Dengue-Associated Acute Kidney Injury. *Am J Trop Med Hyg.* 2021 May 3;105(1):24-30. doi: 10.4269/ajtmh.21-0007. PMID: 33939642; PMCID: PMC8274771.

30. Eswarappa M, Reddy SB, John MM, Suryadevara S, Madhyashatha RP. Renal manifestations of dengue viral infection. *Saudi J Kidney Dis Transpl.* 2019 Mar-Apr;30(2):394-400. doi: 10.4103/1319-2442.256847. PMID: 31031376.

31. Gaut JP, Liapis H. Acute kidney injury pathology and pathophysiology: a retrospective review. *Clin Kidney J.* 2020 Oct 10;14(2):526-536. doi: 10.1093/ckj/sfaa142. PMID: 33623675; PMCID: PMC7886540.
32. Lima EQ, Nogueira ML. Viral hemorrhagic fever-induced acute kidney injury. *Semin Nephrol.* 2008 Jul;28(4):409-415. doi: 10.1016/j.semnephrol.2008.04.009. PMID: 18620963.
33. Paes MV, Pinhão AT, Barreto DF, Costa SM, Oliveira MP, Nogueira AC et al. Liver injury and viremia in mice infected with dengue-2 virus. *Virology.* 2005 Aug 1;338(2):236-46. doi: 10.1016/j.virol.2005.04.042. PMID: 15961136.
34. Barreto DF, Takiya CM, Schatzmayr HG, Nogueira RM, Farias-Filho JC, Barth OM. Histopathological and ultrastructural aspects of mice lungs experimentally infected with dengue virus serotype 2. *Mem Inst Oswaldo Cruz.* 2007 May;102(2):175-82. doi: 10.1590/s0074-02762007005000007. PMID: 17426882.
35. França RF, Zucoloto S, da Fonseca BA. A BALB/c mouse model shows that liver involvement in dengue disease is immune-mediated. *Exp Mol Pathol.* 2010 Dec;89(3):321-6. doi: 10.1016/j.yexmp.2010.07.007. Epub 2010 Jul 29. PMID: 20673760.
36. Salomão NG, Rabelo K, Póvoa TF, Alves AMB, da Costa SM, Gonçalves AJS et al. BALB/c mice infected with DENV-2 strain 66985 by the intravenous route display injury in the central nervous system. *Sci Rep.* 2018 Jun 27;8(1):9754. doi: 10.1038/s41598-018-28137-y. PMID: 29950590; PMCID: PMC6021404.
37. Jácome FC, Teixeira AL, Coutinho DD, Costa AD, Caldas GC, Nunes MA et al. Secondary dengue infection in immunocompetent murine model leads to heart tissue damage. *Acta Virol.* 2019;63(3):292-300. doi: 10.4149/av\_2019\_309. PMID: 31507195.

38. Amorim JFS, Azevedo AS, Costa SM, Trindade GF, Basílio-de-Oliveira CA, Gonçalves AJS et al. Dengue infection in mice inoculated by the intracerebral route: neuropathological effects and identification of target cells for virus replication. *Sci Rep*. 2019 Nov 29;9(1):17926. doi: 10.1038/s41598-019-54474-7. PMID: 31784616; PMCID: PMC6884643.
39. Byrne AB, García AG, Brahamian JM, Mauri A, Ferretti A, Polack FP et al. A murine model of dengue virus infection in suckling C57BL/6 and BALB/c mice. *Animal Model Exp Med*. 2020 Dec 21;4(1):16-26. doi: 10.1002/ame2.12145. PMID: 33738433; PMCID: PMC7954830.
40. Rasinhas AC, Jácome FC, Caldas GC, de Almeida ALT, da Silva MAN, de Souza, DDC et al. Morphological Aspects and Viremia Analysis of BALB/c Murine Model Experimentally Infected with Dengue Virus Serotype 4. *Viruses*. 2021 Sep 29;13(10):1954. doi: 10.3390/v13101954. PMID: 34696384; PMCID: PMC8538460.
41. Jácome FC, Caldas GC, Rasinhas AC, de Almeida ALT, de Souza DDC, Paulino AC et al. Immunocompetent Mice Infected by Two Lineages of Dengue Virus Type 2: Observations on the Pathology of the Lung, Heart and Skeletal Muscle. *Microorganisms*. 2021 Dec 8;9(12):2536. doi: 10.3390/microorganisms9122536. PMID: 34946137; PMCID: PMC8704795.
42. Jácome FC, Caldas GC, Rasinhas AC, de Almeida ALT, de Souza DDC, Paulino AC et al. Comparative analysis of liver involvement caused by two DENV-2 lineages using an immunocompetent murine model. *Sci Rep*. 2021 May 6;11(1):9723. doi: 10.1038/s41598-021-88502-2. PMID: 33958631; PMCID: PMC8102549.
43. Kangussu LM, Costa VV, Olivon VC, Queiroz-Junior CM, Gondim ANS, Melo MB et al. Dengue virus infection induces inflammation and oxidative stress on the heart. *Heart*. 2022 Mar;108(5):388-396. doi: 10.1136/heartjnl-2020-318912. Epub 2021 May 28. PMID: 34049953.

44. Balmaseda A, Hammond SN, Pérez L, Tellez Y, Saborío SI, Mercado JC et al. Serotype-specific differences in clinical manifestations of dengue. *Am J Trop Med Hyg.* 2006 Mar;74(3):449-56. PMID: 16525106.
45. Barreto DF, Takiya CM, Paes MV, Farias-Filho J, Pinhão AT, Alves AM et al. Histopathological aspects of Den-gue-2 virus infected mice tissues and complementary virus isolation. *J Submicrosc Cytol Pathol.* 2004 Apr;36(2):121-30. PMID: 15554498.
46. Jácome FC, Caldas GC, Rasinhas AC, de Almeida ALT, de Souza DDC, Paulino AC et al. Brazilian Dengue Virus Type 2-Associated Renal Involvement in a Murine Model: Outcomes after Infection by Two Lineages of the Asian/American Genotype. *Pathogens.* 2021 Aug 26;10(9):1084. doi: 10.3390/pathogens10091084. PMID: 34578117; PMCID: PMC8467194.
47. Johnson BW, Russell BJ, Lanciotti RS. Serotype-specific detection of dengue viruses in a fourplex real-time reverse transcriptase PCR assay. *J Clin Microbiol.* 2005; 43(10):4977–4983.
48. Igarashi A. Isolation of a Singh's *Aedes albopictus* cell clone sensitive to Dengue and Chikungunya viruses. *J Gen Virol.* 1978 Sep;40(3):531-44. doi: 10.1099/0022-1317-40-3-531. PMID: 690610.
49. Reed LJ, Muench H. A simple method of estimating fifty per cent endpoints. *Am J Epidemiol.* 1938; 27(3):493-497.
50. Barreto-Vieira DF, Barth-Schatzmayr OM, Schatzmayr HG. Modelo animal experimental para o estudo da patogênese dos vírus dengue sorotipos 1 e 2. Manual de técnicas, 1st ed. Interciência: Rio de Janeiro, Brazil, 2010.

51. Gurugama P, Jayarajah U, Wanigasuriya K, Wijewickrama A, Perera J, Seneviratne SL. Renal manifestations of dengue virus infections. *J Clin Virol.* 2018 Apr;101:1-6. doi: 10.1016/j.jcv.2018.01.001. Epub 2018 Jan 6. PMID: 29414180.
52. U.S. Department of Health and Human Services. National Toxicology Program. NTP Nonneoplastic Lesion Atlas. [updated 2014 October 23; cited 2022 August 31] Available from: <https://ntp.niehs.nih.gov/nnl/urinary/kidney/rtvac/index.htm>.
53. Boonpucknavig S, Vuttiviroj O, Boonpucknavig V. Infection of young adult mice with dengue virus type 2. *Trans R Soc Trop Med Hyg.* 1981;75(5):647-53. doi: 10.1016/0035-9203(81)90142-5. PMID: 7036427.
54. Lizarraga KJ, Nayer A. Dengue-associated kidney disease. *J Nephropathol.* 2014;3(2):57-62. doi: 10.12860/jnp.2014.13. Epub 2013 Dec 28. PMID: 24772398; PMCID: PMC3999585.
55. Wiwanitkit V. Immune complex: does it have a role in pathogenesis of renal failure in dengue infection? *Ren Fail.* 2005;27(6):803-4. doi: 10.1080/08860220500244914. PMID: 16350839.
56. Lien TS, Sun DS, Wu CY, Chang HH. Exposure to Dengue Envelope Protein Domain III Induces Nlrp3 Inflammasome-Dependent Endothelial Dysfunction and Hemorrhage in Mice. *Front Immunol.* 2021 Feb 25;12:617251. doi: 10.3389/fimmu.2021.617251. PMID: 33717109; PMCID: PMC7947687.
57. Basu A, Jain P, Sarkar P, Gangodkar S, Deshpande D, Ganti K et al. Dengue virus infection of SK Hep1 cells: inhibition of in vitro angiogenesis and altered cytomorphology by expressed viral envelope glycoprotein. *FEMS Immunol Med Microbiol.* 2011 Jul;62(2):140-7. doi: 10.1111/j.1574-695X.2011.00794.x. Epub 2011 Mar 16. PMID: 21332827.

58. Castillo JA, Naranjo JS, Rojas M, Castaño D, Velilla PA. Role of Monocytes in the Pathogenesis of Dengue. *Arch Immunol Ther Exp (Warsz)*. 2019 Feb;67(1):27-40. doi: 10.1007/s00005-018-0525-7. Epub 2018 Sep 20. PMID: 30238127.
59. Fink J, Gu F, Vasudevan SG. Role of T cells, cytokines and antibody in dengue fever and dengue haemorrhagic fever. *Rev Med Virol*. 2006 Jul-Aug;16(4):263-75. doi: 10.1002/rmv.507. PMID: 16791836.
60. Srikiatkachorn A, Mathew A, Rothman AL. Immune-mediated cytokine storm and its role in severe dengue. *Semin Immunopathol*. 2017 Jul;39(5):563-574. doi: 10.1007/s00281-017-0625-1. Epub 2017 Apr 11. PMID: 28401256; PMCID: PMC5496927.
61. Oliveira LLS, Alves FAV, Rabelo K, Moragas LJ, Mohana-Borges R, de Carvalho JJ et al. Immunopathology of Renal Tissue in Fatal Cases of Dengue in Children. *Pathogens*. 2022 Dec 15;11(12):1543. doi: 10.3390/pathogens11121543. PMID: 36558877; PMCID: PMC9785549.
62. Laoprasopwattana K, Pruekprasert P, Dissaneewate P, Geater A, Vachvanichsanong P. Outcome of dengue hemorrhagic fever-caused acute kidney injury in Thai children. *J Pediatr*. 2010 Aug;157(2):303-9. doi: 10.1016/j.jpeds.2010.02.008. Epub 2010 Apr 1. PMID: 20362302.
63. Imad HA, Phumratanapapin W, Phonrat B, Chotivanich K, Charunwatthana P, Muangnoicharoen S et al. Cytokine Expression in Dengue Fever and Dengue Hemorrhagic Fever Patients with Bleeding and Severe Hepatitis. *Am J Trop Med Hyg*. 2020 May;102(5):943-950. doi: 10.4269/ajtmh.19-0487. PMID: 32124729; PMCID: PMC7204576.
64. Rajan M, Geminiganesan S, Sankaranarayanan S, Padmanaban R, Selvam MP. Renal Manifestations in Children with Dengue Fever Hospitalized in Pediatric Intensive Care Unit. *Indian*

J Pediatr. 2020 Dec;87(12):1014-1017. doi: 10.1007/s12098-020-03402-z. Epub 2020 Jun 15. PMID: 32557142.

**Table I.** Frequency of histopathological alterations observed in the kidneys of BALB/c mice infected with DENV-4.

<b>Histopathological Alteration</b>	<b>Positive/Tested (%)</b>
Tubular necrosis	9/10 (90)
Inflammatory cell infiltrate	8/10 (80)
Glomerular enlargement	8/10 (80)
Cytoplasmic vacuoles	5/10 (50)
Erythrocytes in the Bowman's space	5/10 (50)
Hemorrhage	4/10 (40)
Capillary edema	2/10 (20)



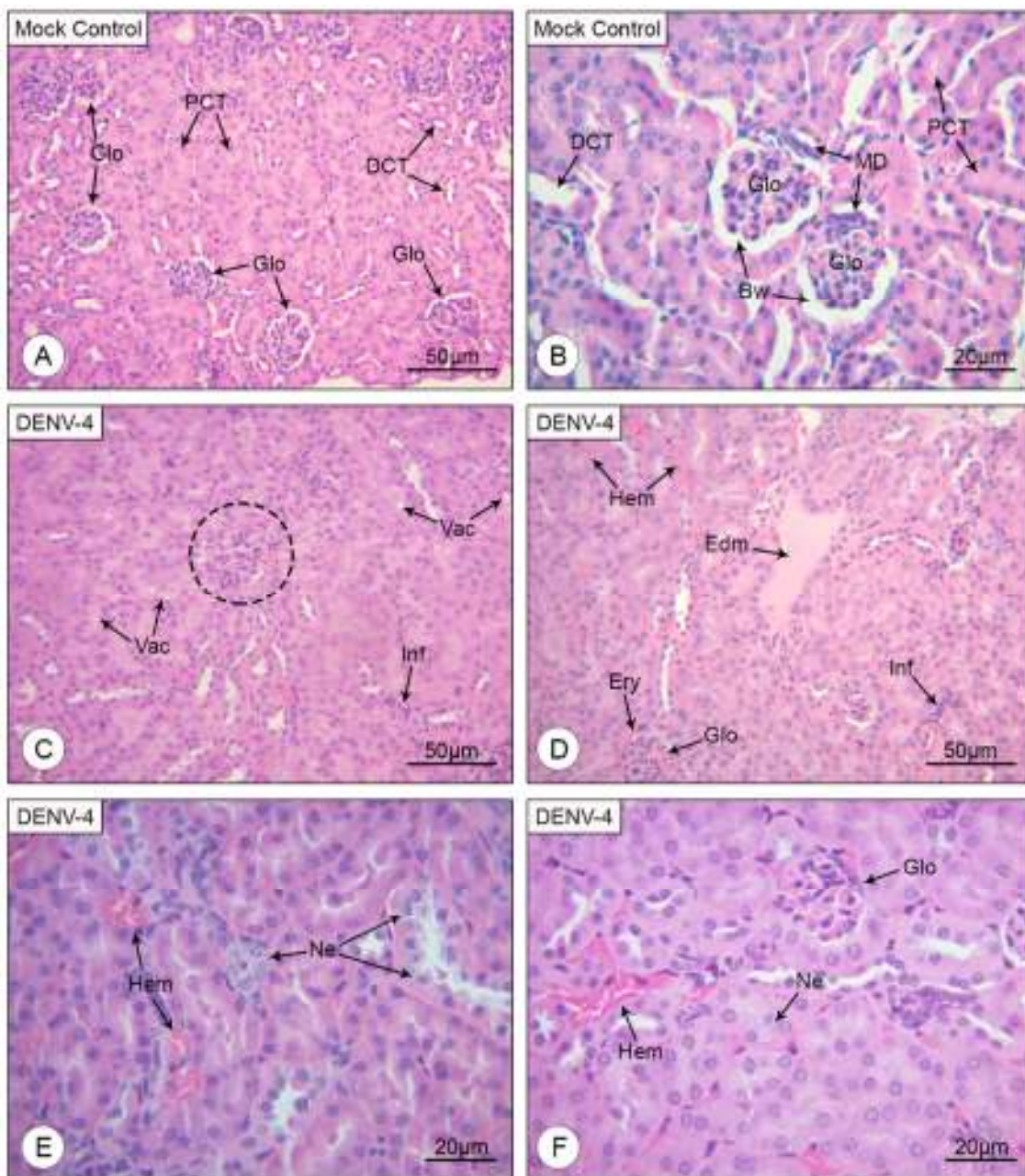


**Figure 1.** Histological sections of BALB/c mice kidney stained with H&E (A, B: Uninfected mice; C-F: DENV-4 infected mice). (A, B) Glomerulus (Glo); Distal convoluted tubule (DCT); Proximal convoluted tubule (PCT); Bowman's space (Bw); Macula densa (MD). (C) Glomerulus presenting reduced Bowman's space (dashed outline); Tubular cells containing cytoplasmic vacuoles (Vac); Inflammatory infiltrate (Inf). (D) Areas of interstitial hemorrhage (Hem); Capillary edema (Edm);

Erythrocytes in the Bowman's space (Ery) of the Glomerulus (Glo); Inflammatory infiltrate (Inf). (E, F) Areas of interstitial hemorrhage (Hem); Tubular necrosis (Ne); Glomerulus (Glo). Magnification: (A, C, D) 200x; (B, E, F) 400x.

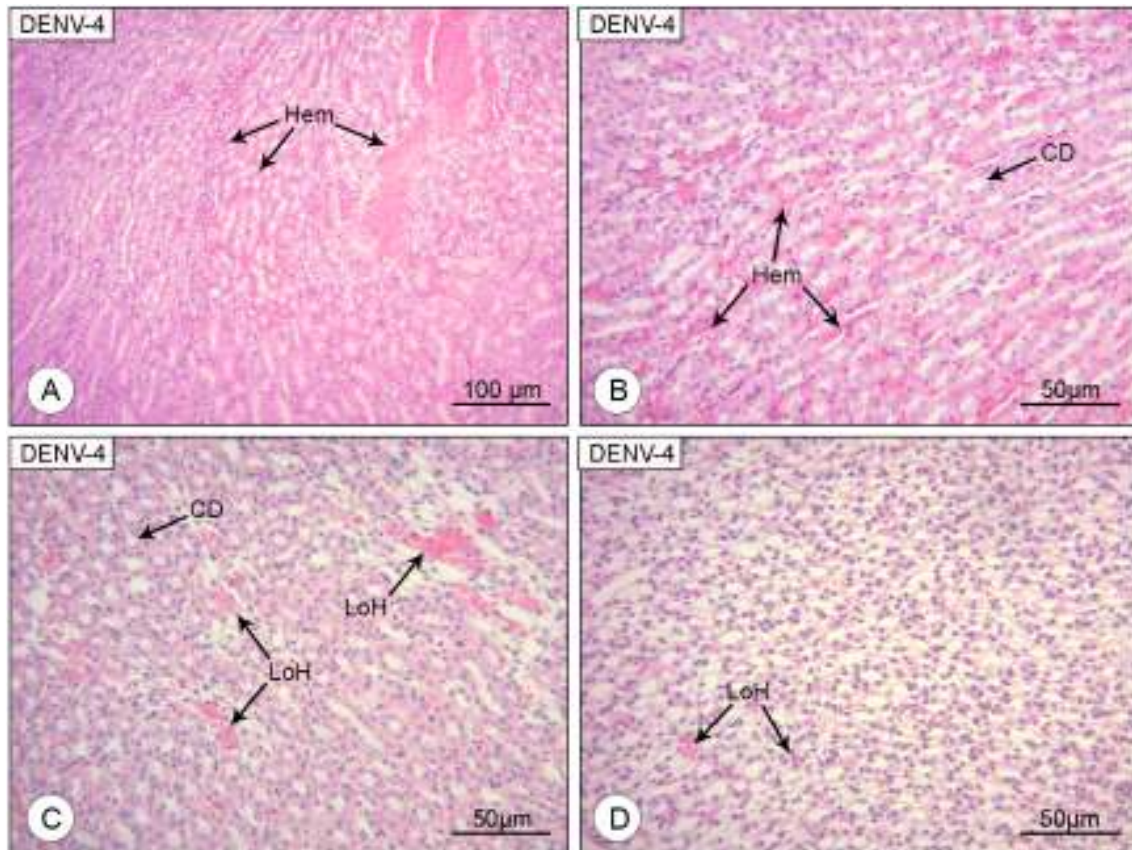


**Figure 2.** Histological sections of DENV-4 infected BALB/c mice kidney stained with H&E. (A, B) Areas of interstitial hemorrhage (Hem); Collecting duct (CD). (C, D) Thin part of the loop of Henle containing blood (LoH); Collecting duct (CD). Magnification: (A) 100x; (B, C, D) 200x.

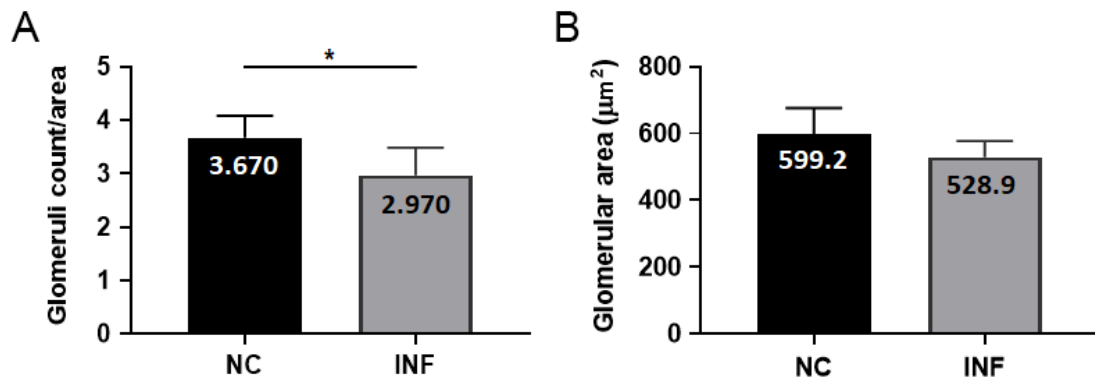


**Figure 3.** Glomeruli count per analysed area (**A**) and mean area occupied by glomeruli (**B**) of negative control (NC) and DENV-4 infected (INF) BALB/c mice. \*:  $p < 0.05$ .

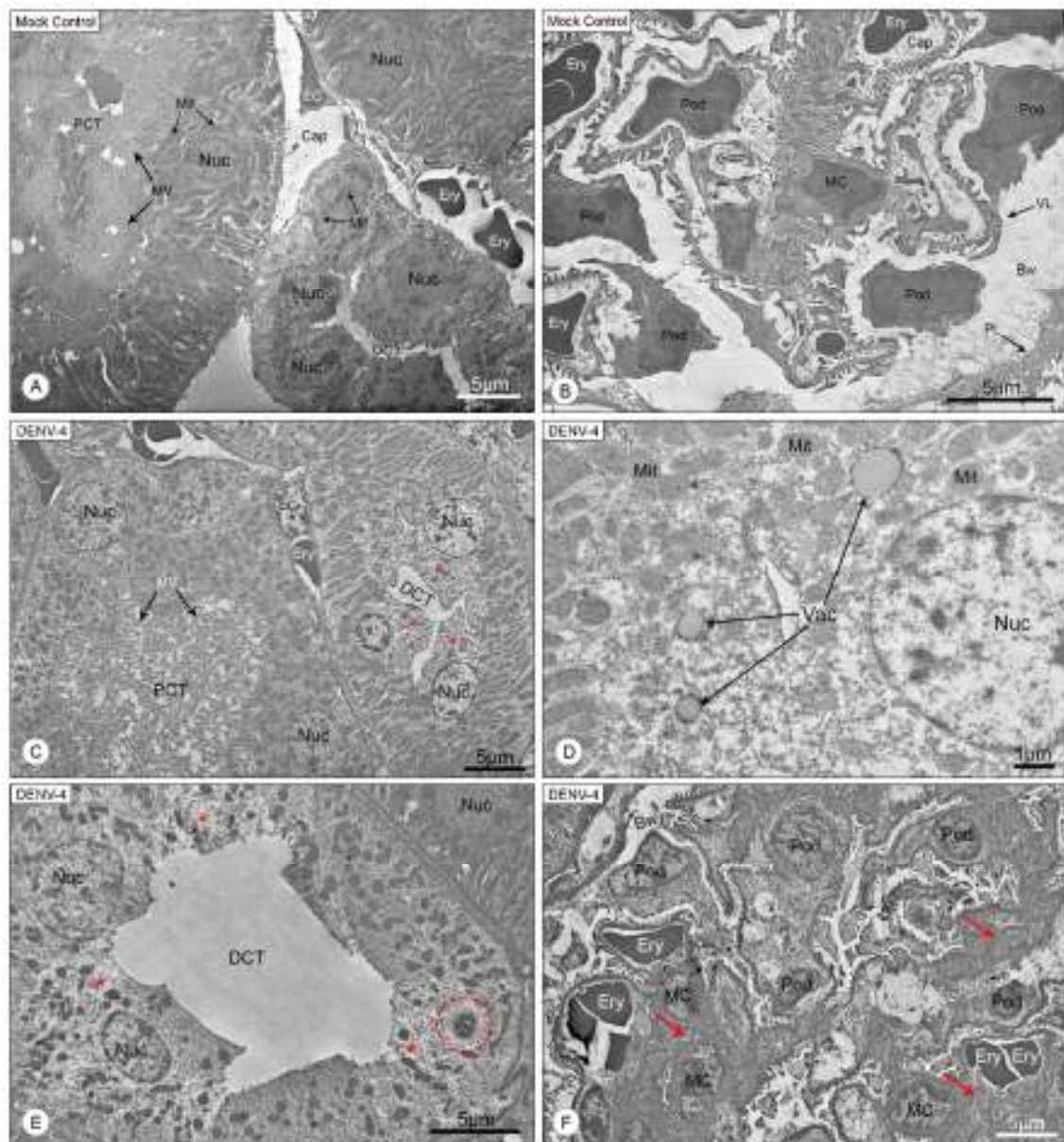


**Figure 4.** Electron micrographs of BALB/c mice kidney sections (A, B: Uninfected mice; C-F: DENV-4 infected mice). **(A)** Proximal convoluted tubule (PCT); Microvilli (MV) that form the brush border; Nucleus (Nuc); Distal convoluted tubule (DCT); Mitochondrion (Mit); Endothelial cell (EC) that forms the capillary (Cap); Erythrocytes (Ery). **(B)** Podocytes (Pod) that surround the glomerular capillaries (Cap); Mesangial cell (MC); Visceral layer (VL) and parietal layer (PL) of the Bowman's space (Bw); Erythrocytes (Ery). **(C)** Cells of the distal convoluted tubule (DCT) presenting loss of cytoplasm (\*); Nucleus (Nuc); Proximal convoluted tubule (PCT) showing loss of microvilli (MV).

**(D)** Vacuoles (Vac) of indistinct origin in the cytoplasm of a distal tubular cell; Nucleus (Nuc); Mitochondrion (Mit). **(E)** Cells of the distal convoluted tubule (DCT) presenting loss of cytoplasm (\*) and pyknotic nucleus (red dashed outline); Nucleus (Nuc). **(F)** Reduced Bowman's space (Bw); Podocytes (Pod); Mesangial cells (MC) presenting expanded mesangial matrix (red arrow); Erythrocytes (Ery). Magnification: (A, C) 1.200x; (B, E, F) 1.500x; (D) 2.500x.

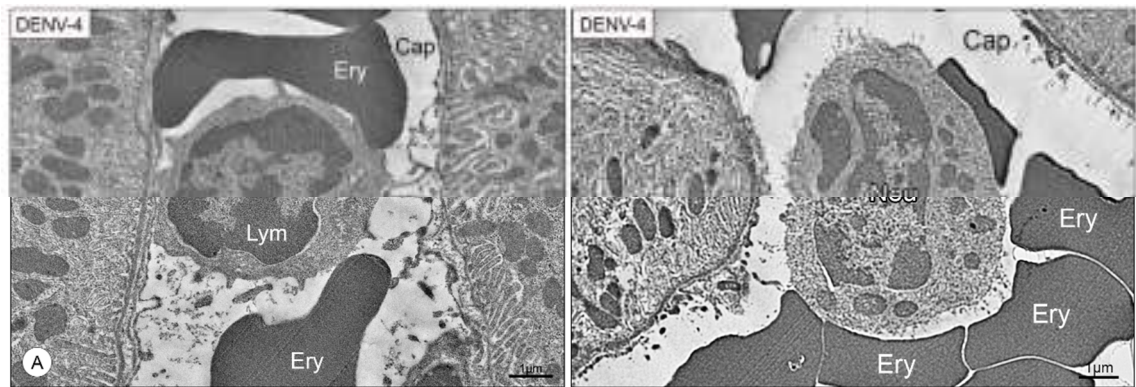


**Figure 5.** Electron micrographs of DENV-4 infected BALB/c mice kidney sections. **(A)** Lymphocyte (Lym) circulating in a capillary (Cap); Erythrocyte (Ery). **(B)** Neutrophil (Neu) circulating in the capillary; Erythrocyte (Ery). (Cap). Magnification: (A) 6.000x (B) 2.000x.

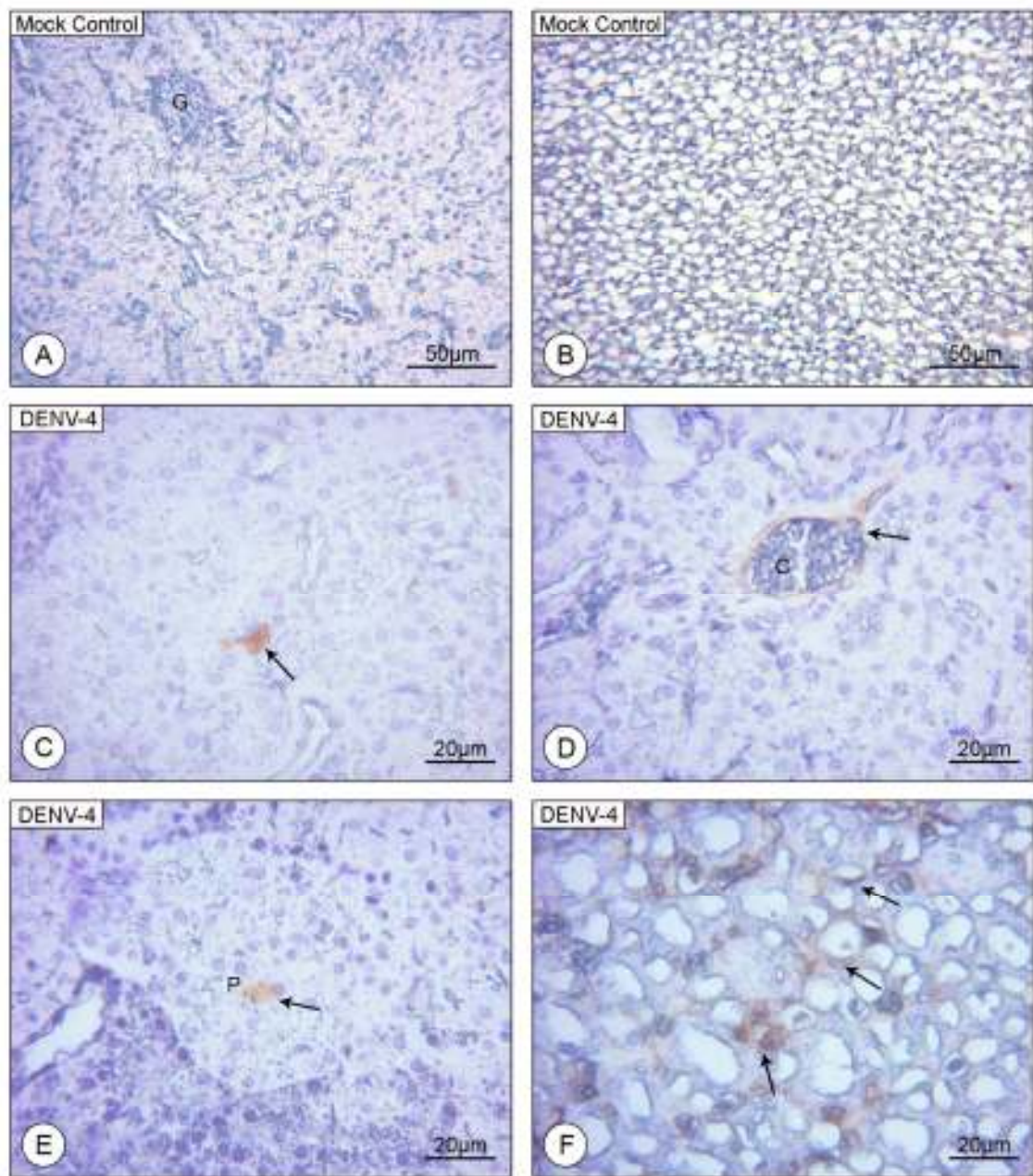


**Figure 6.** Histological sections of BALB/c mice kidney counterstained with Harris Hematoxylin (A, B: Uninfected mice; C-F: DENV-4 infected mice) (A, B) Kidney sections showing no peroxidase reactive cells; Glomerulus (G). (C) Envelope protein reactive tubular cell (arrow). (D) Envelope protein reactive endothelium (arrow). (E) Envelope protein reactive lumen (arrow) of the proximal convoluted tubule (P). (F) Envelope protein reactive cells of the loop of Henle (arrow). Magnification: (A, B) 200x; (C, D, E, F) 400x.